Interactions of Protons with Single Open L-Type Calcium Channels

Location of Protonation Site and Dependence of Proton-induced Current Fluctuations on Concentration and Species of Permeant Ion

BLAISE PROD'HOM, DANIELA PIETROBON, AND PETER HESS

From the Department of Cellular and Molecular Physiology, and the Program in Neuroscience, Harvard Medical School, Boston, Massachusetts 02115

ABSTRACT We further investigated the rapid fluctuations between two different conductance levels promoted by protons when monovalent ions carry current through single L-type Ca channels. We tested for voltage dependence of the proton-induced current fluctuations and for accessibility of the protonation site from both sides of the membrane patch. The results strongly suggest an extracellular location of the protonation site. We also studied the dependence of the kinetics of the fluctuations and of the two conductance levels on the concentration of permeant ion and on external ionic strength. We find that saturation curves of channel conductance vs. [K] are similar for the two conductance levels. This provides evidence that protonation does not appreciably change the surface potential near the entry of the permeation pathway. The proton-induced conduction change must therefore result from an indirect interaction between the protonation site and the ion-conducting pathway. Concentration of permeant ion and ionic strength also affect the kinetics of the current fluctuations, in a manner consistent with our previous hypothesis that channel occupancy destabilizes the low conductance channel conformation. We show that the absence of measurable fluctuations with Li and Ba as charge carriers can be explained by significantly higher affinities of these ions for permeation sites. Low concentrations of Li reduce the Na conductance and abbreviate the lifetimes of the low conductance level seen in the presence of Na. We use whole-cell recordings to extrapolate our findings to the physiological conditions of Ca channel permeation and conclude that in the presence of 1.8 mM Ca no proton-induced fluctuations occur between pH 7.5 and 6.5. Finally, we propose a possible physical interpretation of the formal model of the protonation cycle introduced in the companion paper.

Address reprint requests to Dr. Peter Hess, Department of Cellular and Molecular Physiology, Harvard Medical School, 25 Shattuck Street, Boston, MA 02115. Dr. Prod'hom's present address is Department of Chemistry, Harvard University, Cambridge, MA 02138. Dr. Pietrobon's permanent address is Department of General Pathology, University of Padova, 35100 Padova, Italy.

J. GEN. PHYSIOL. © The Rockefeller University Press · 0022-1295/89/07/0023/20 $2.00 23
Volume 94 July 1989 23–42

INTRODUCTION

In the preceding paper (Pietrobon et al., 1989), we have presented a quantitative analysis of the proton-induced current fluctuations of the dihydropyridine (DHP)-sensitive (L-type) Ca channel with monovalent ions as charge carriers. In this paper we investigate the location of the protonation site, the interactions between the protonation site and permeant ions binding to intra-channel binding sites, and the effects of changes in ionic strength. We extend our measurements to permeant ions that resemble the physiological charge carrier, Ca, more closely, in an effort to judge the importance of proton-induced current fluctuations under physiological conditions of Ca channel permeation.

We conclude that the protonation site is located at the external surface of the channel protein. It is situated far enough from the permeation pathway, such that permeant ions entering the channel do not experience direct electrostatic effects from the presence of the proton. We confirm our previous hypothesis (Pietrobon et al., 1988) that occupancy of the channel by a permeant ion destabilizes the conformation in which the protonation site binds the proton tightly. Permeant ions with high affinity to the permeation path greatly disfavor the low conductance conformation, such that with physiological external solutions no reduction of the channel conductance by protons is observed. We discuss a possible physical interpretation of the formal model introduced in the companion paper (Pietrobon et al., 1989).

METHODS

The methods for obtaining single-cell preparations, recording and analysis of single-channel currents were as described in Pietrobon et al. (1989). Cell-attached and inside-out patch recordings (Hamill et al., 1981) were obtained from freshly dissociated guinea pig ventricular myocytes or undifferentiated PC-12 cells. Single L-type Ca channels were identified by their voltage dependence, conductance, and sensitivity to the DHP Ca channel agonist (+)-S-202-791 (a gift from Dr. Hof, Sandoz Co., Basle, Switzerland), which was present at 0.5–1 μM in all single-channel experiments.

For cell-attached recordings with monovalent charge carriers the pipette solution contained 150 mM of the Cl-salt of Li, Na, or K, 5 mM EDTA, and 5 mM of the pH buffer MES (pK 6.15), HEPES (pK 7.55), or TAPS (pK 8.4). The solutions were titrated to the desired pH with LiOH, NaOH, or KOH. Thus the final pipette concentration of cation was ~160 mM. Concentrations of cations were reduced by substitution on an osmole for osmole basis with either choline-Cl, tetraethylammonium chloride (TEA-Cl), or sucrose. Solutions in D_2O (Aldrich Chemical Co., Milwaukee, WI) were similar, the slight contamination by protons from the pH buffers added at 5 mM was judged insignificant. pD values were obtained on a regular pH meter calibrated with pH buffers by the convention pD = meter reading + 0.4 (Perrin and Dempsey, 1974). For experiments with Ba as the charge carrier, the pipette contained 110 mM $BaCl_2$ and 5 mM of one of the pH buffers listed above. In all cell-attached recordings, the bathing solution was the high K solution used to zero the cell membrane potential outside the patch. It contained (in millimolar): 140 K-aspartate, 10 EGTA, 10 HEPES, and 20 $MgCl_2$, titrated to pH 7.4 with KOH.

Inside-out patches were excised into a Ca- and Mg-free solution containing 140 Na-aspartate, 10 mM EDTA, and 5 mM HEPES, titrated to pH 7.5. The pipette solutions for inside-out patches were similar to those used for cell-attached recordings, except that Cl ions were replaced by aspartate ions.

RESULTS

Kinetics of Proton-induced Fluctuations Are Voltage Independent

In an attempt to situate the protonation site with respect to the transmembrane electric field, we studied the kinetics of the transitions between the two conductance levels at different potentials. Fig. 1 shows histograms of dwell times at the two current levels obtained in the same patch at −70 and −120 mV. The two corresponding histograms at each potential are superimposed and it is clear that they are very similar and the mean dwell times obtained as the time constants of the fitted exponentials are indistinguishable. The results shown in Fig. 1 were obtained with K as the charge carrier, but lack of voltage dependence of the kinetics of proton-induced fluctuations was also observed with Cs or Na as permeant ions (data not shown). Even though there is no simple relationship between the protonation/deproton-

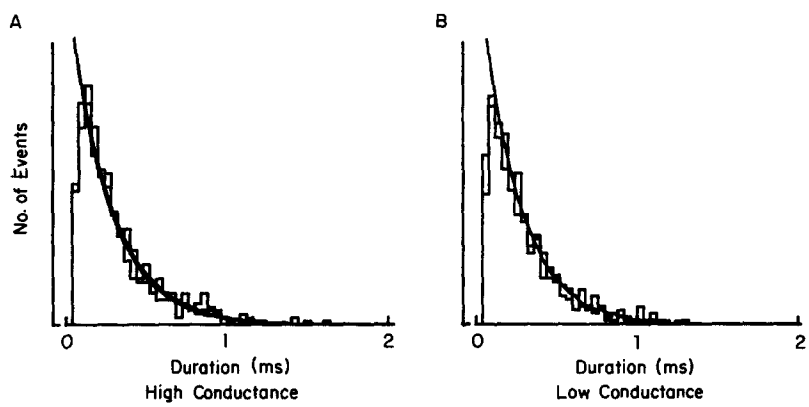

FIGURE 1. Kinetics of proton-induced fluctuations are voltage independent. Distributions of dwell times at the high (*A*) and low (*B*) conductance level. Histograms obtained at −70 and −120 mV are superimposed. Mean durations are 0.24 ms at both voltages at the high conductance and 0.26 ms (−70 mV) and 0.25 ms (−120 mV) at the low conductance. Cell-attached recording. Pipette solution, 160 mM K.

ation events and the mean dwell times at the two conductance levels (Pietrobon et al., 1989), the voltage independence of the kinetics strongly suggests that the protonation and deprotonation events occur outside the transmembrane electric field (see Discussion). Thus we conclude that the protonation site is located at the external surface of the channel protein. Moreover, the conformational change underlying the conductance change (Pietrobon et al., 1988, 1989) seems not to move net charge within the electric field.

Permeation of Monovalent Ions through L-Type Ca Channels is Asymmetric

The presence of this external protonation site raises the question of whether a similar site exists on the internal channel surface or whether L-type Ca channels are functionally and structurally asymmetrical as far as their permeation properties are concerned. Previous studies have failed to demonstrate functional asymmetry in L-

type Ca channels (Rosenberg et al., 1986). We therefore measured inward and outward currents carried by monovalent ions in inside-out patches where both the external and internal pH were under our experimental control. In confirmation of most previous studies (e.g., Fenwick et al., 1982; Cavalie et al., 1983; Nilius et al., 1985; Yatani et al., 1987) we found that L-type Ca channels remain active in excised patches for only very brief periods of time, ranging from seconds to a few minutes at best. Nevertheless, we were able to establish the pattern of currents shown in Fig. 2. To observe long-lasting outward currents through L-type Ca channels, we had to eliminate all internal divalent ions with the use of EDTA. In the presence of internal Mg, only flickery outward channel openings were observed, which is consistent with open channel block by internal Mg. We used Cl-free solutions to exclude the possibility of overlapping outward Cl currents.

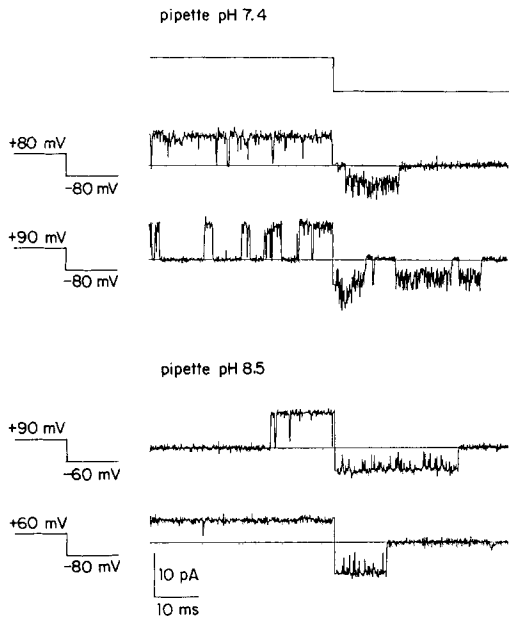

FIGURE 2. Current fluctuations of inward currents correlate with pH_o, not pH_i. Inside-out patch. Symmetrical 160 mM Na-aspartate. pH_o = 7.4 (*top*) and 8.5 (*bottom*). pH_i = 7.5 for both conditions. Pulse protocol is shown on the top of the traces with individual potential values shown on the left of each trace. Linear components of leak and capacitance subtracted digitally. Inside-out patch recordings.

Fig. 2 shows current traces in an inside-out patch in response to voltage-clamp depolarizations from negative to positive potentials. In the example shown, the pipette and bath solutions each contain 160 mM of Na as the only cation. The depolarization opens a channel that carries outward current at +80 mV. The channel remains open for several tens of milliseconds after repolarization and carries inward current at the negative potential. The inward current shows the characteristic fast open channel noise expected at a pipette pH of 7.4 with Na as the charge carrier (Prod'hom et al., 1987; Pietrobon et al. 1988, 1989). In contrast, the outward currents during the depolarization show significantly less open channel noise, despite symmetrical proton activities on either side of the patch. The lower traces in Fig. 2 show that at constant internal pH (pH_i) the noise of the inward current varies as expected with the pipette pH (pH_o), whereas the outward currents are little affected by the change in pH_o. The proton-induced fluctuations were similar in experiments

in which pH_i was either 7.5 or 8.5. Thus, proton-induced fluctuations correlated with pH_o, not pH_i. Internal protons therefore do not seem to have access to the external protonation site and there does not seem to be a corresponding site on the inner channel surface. No clear current fluctuations are seen in the outward currents, although comparison of the traces at pH_o 7.4 and 8.5 suggests a slight increase in the open channel noise of the outward currents at pH_o 7.4. Thus Na ions moving from inside to outside may also experience the difference in channel conformation promoted by external protons, but clearly the conformational change affects Na permeation in a very asymmetrical way.

Protonation Does Not Change the Negative Surface Potential Near the Entry of the Conduction Pathway

If the protonation site is situated close enough to the external mouth of the permeation pathway, one would predict that the altered local surface potential associated

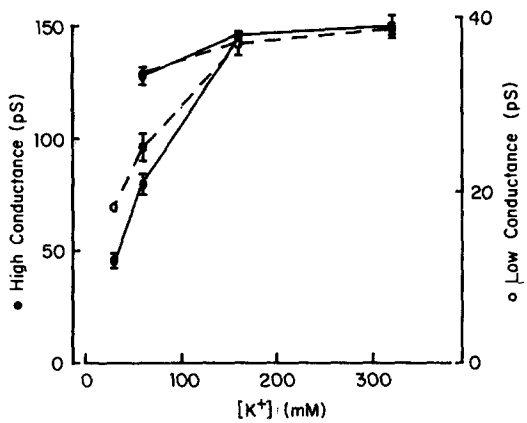

FIGURE 3. Conductance-concentration plots are similar for the high and low conductance levels. Single-channel conductances as a function of [K], obtained by linear regression of the inward currents between −120 and −30 mV. Filled symbols (mean ± SEM) joined by a solid line, high conductance. Empty symbols joined by a dashed line, low conductance. Both conductances were measured at pH 8.4. The higher values at 60 mM K were obtained with 60 mM KCl + 200 mM sucrose, the lower values were obtained with 60 mM KCl + 100 mM choline-Cl. The points at 30 mM K were measured in the presence of 130 mM choline. Cell-attached patches.

with the protonated and unprotonated states would change the local concentration of permeant ions (see e.g., Dani, 1986; Prod'hom et al., 1987). We tested this hypothesis by studying the dependence of the conductance on the bulk [K] for the high and low conductance states separately.

Fig. 3 shows that the saturation curves of the two conductances with increasing [K] are quite similar, both under conditions of constant ionic strength (K replaced by choline) or varying ionic strength (K replaced by sucrose). Thus the protonated state does not reduce the channel conductance by making the surface potential near the channel entrance more positive, since in that case one would expect a shift of the half-saturation point towards higher bulk [K] for the low conductance (mainly protonated) state of the channel.

However, there is clear evidence for the existence of net negative charge near the

permeation pathway since in Fig. 3 the conductance starts to decrease at higher bulk [K] when ionic strength is kept constant with choline. This is the expected result if a negative surface potential increases the local [K] at the pore entrance above the bulk [K]. The decrease of ionic strength in 60 mM KCl + sucrose would increase the negative surface potential and the ratio of mouth [K]/bulk [K], and therefore counteract the decrease in conductance found at lower bulk [K] with constant ionic strength (see e.g., Apell et al., 1979; Wilson et al., 1983; Cota and Stefani, 1984; Coronado and Affolter, 1986; Dani, 1986; Dani and Eisenman, 1987). An alternative explanation would be that choline blocks the channel, rather than reducing the conductance by screening negative surface charge. This is unlikely because the current-voltage relations in the presence and absence of choline are linear. Therefore, choline reduces the conduction in a non–voltage-dependent way that seems incompatible with block by a charged molecule. Substitution of permeant ions by TEA and choline gave similar results (see Fig. 4).

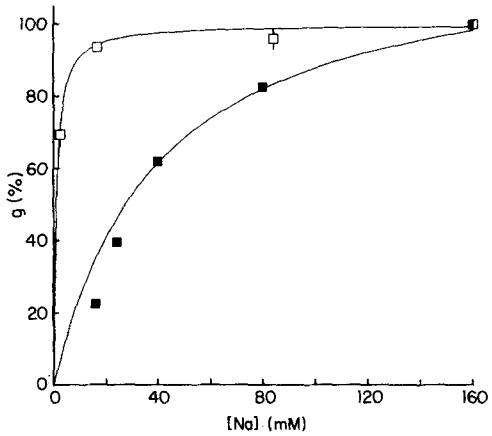

FIGURE 4. Ionic strength influences saturation curves for Na conductance at pH 9. Normalized sodium conductance at pH 9 as a function of pipette [Na]. Sodium in the pipette is substituted by TEA (*closed squares*) or sucrose (*open squares*). Standard error of the mean (SEM) shown for points with more than two measurements. SEM for point at 160 mM Na is smaller than symbol size. All conductances are normalized to the value with 160 mM [Na]. Cell-attached patches.

We conclude from Fig. 3 that there is a negative surface potential that is felt by permeant ions entering the channel but that the protonation site does not significantly alter this potential. Thus the protonation site cannot be located directly at the entrance of the permeation pathway and must influence the conductance indirectly by an allosteric mechanism.

The presence of negative surface charge is further emphasized when we consider the plot of conductance vs. [Na] shown in Fig. 4. The values in Fig. 4 were obtained at pH 9 and therefore represent the high conductance. Again we see a striking difference between the closed symbols, obtained at constant ionic strength (Na replaced by TEA), and the open symbols, which represent experiments in which ionic strength decreased as sucrose was substituted for Na.

Another important conclusion is apparent from comparison of Figs. 3 and 4: the point of half saturation for Na is ~40 mM at constant ionic strength, while it is ~60 mM for K. This is consistent with a higher affinity of Na than K for an intra-channel binding site, a conclusion which we had previously reached based on unitary con-

ductance and extrapolated reversal potentials (Pietrobon et al., 1988). The same sequence of affinities for monovalent ions is also found in skeletal muscle T tubular Ca channels (Coronado and Smith, 1987), but the two channel types differ significantly in other aspects of their permeability to monovalent cations (see Discussion).

We have superimposed rectangular hyperbolas on the experimental points in Fig. 4. This mainly serves to emphasize qualitatively the dramatic difference in the saturation behavior with constant or varying ionic strength and to allow an estimate of the half-saturation point. We do not mean to imply that the curves should actually fit a rectangular hyperbola, since that would only be expected for one-site channels in the presence of a constant surface potential (see e.g., Coronado and Affolter, 1986).

Mixtures of Na and Li: Mole Fraction Effect and Kinetics of Proton-induced Fluctuations

One intriguing finding remains the absence of proton-induced fluctuations when Li ions carry currents through L-type Ca channels (Hess et al., 1986). This could indicate a specific interaction between Li and the protonation site, but a more attractive hypothesis is that the lack of observable proton-induced fluctuations is related to a much higher affinity of Li for the permeation sites, which would tend to destabilize the low conductance states (Pietrobon et al., 1988).

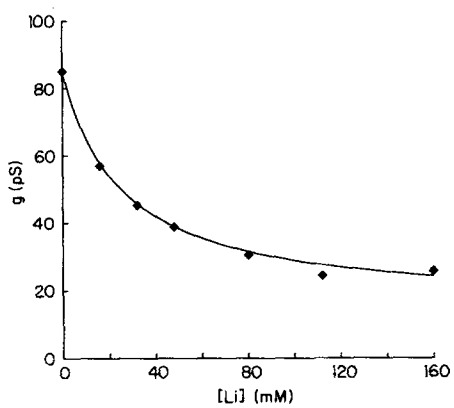

FIGURE 5. Single-channel conductance of Na-Li mixtures at pH 9. [Li] + [Na] = 160 mM. The solid line is a fit to Eq. 1 obtained with $K_{m,Na}$ = 40 mM and $K_{m,Li}$ = 4.5 mM. Cell-attached patches.

To estimate the relative affinities of Li and Na to the permeation path of the L-type Ca channel, we measured the conductances of the linear part of the inward currents carried by mixtures of Li and Na where [Li] + [Na] = 160 mM. The result of this mole fraction experiment is shown in Fig. 5. As the Li mole fraction increases, the conductance decreases and reaches a value of ~25 pS in 100% Li. The conductance in none of the mixtures is smaller than the conductance in Li or Na alone, indicating the absence of an "anomalous mole fraction effect" (Eisenman et al., 1967), which would have pointed to interactions between the two ions in a multiply occupied pore (Hille and Schwarz, 1978; Urban et al., 1987). Thus, contrary to Ca and Ba (Almers and McCleskey, 1984; Hess and Tsien, 1984); which occupy L-

type Ca channels at more than one site, the permeation of Li and Na ions probably involves mainly single occupancy of the channel. We fitted a curve to the data in Fig. 5 which describes the measured total conductance g_t in a one-site pore for which the two ions compete (see e.g., Hille, 1984).

$$g_t = [g_{Li}([Li]/K_{m,Li}) + g_{Na}([Na]/K_{m,Na})]/[1 + ([Li]/K_{m,Li}) + ([Na]/K_{m,Na})] \quad (1)$$

g_{Li} and g_{Na} are the maximal conductances in Li and Na alone. $K_{m,Li}$ and $K_{m,Na}$ are the dissociation constants between the two ions and the site in the pore. With the values for g_{Na} = 106 pS and $K_{m,Na}$ = 40 mM derived from Fig. 4, and g_{Li} = 25 pS, we obtained a very reasonable fit to the data in Fig. 5 with a value of $K_{m,Li}$ = 4.5 mM. The important point here is not to get a precise value for the affinity of Li for a channel site, but to estimate the relative affinities of Li and Na, which turns out to be ~9. It is clear that Li binds significantly stronger than Na. Equal affinities for Na and Li ($K_{m,Li} = K_{m,Na}$) would be indicated by a straight line connecting the conductance in Na alone to that in Li alone. Any set of data points falling below that line means higher affinity for Li than for Na.

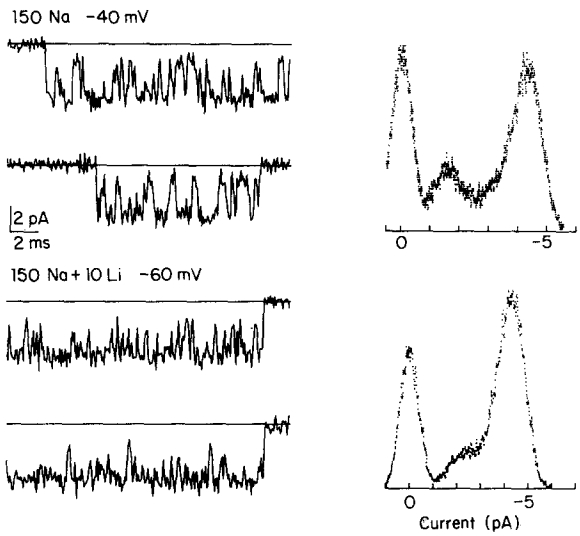

FIGURE 6. Li shortens the dwell times at the low conductance level in the presence of Na. Cell-attached recordings with D_2O in the pipette. pD = 8.2. 150 mM Na + 0 Li at −40 mV (two top traces) and 150 mM Na + 10 mM Li at −60 mV (two bottom traces). Corresponding amplitude histograms in right panels.

The conclusion that Li binds more strongly than Na is consistent with results of reversal potentials under bi-ionic conditions in L-type Ca channels in heart (Hess et al., 1986) skeletal muscle T-tubular Ca channels (Coronado and Smith, 1987), and (T type?) Ca channels in myeloma cells (Fukushima and Hagiwara, 1985).

Fig. 6 tests the hypothesis that Li destabilizes the low conductance level more than Na. To resolve the proton-induced fluctuations with Na as permeant ion, the experiments were carried out in D_2O, which prolongs the lifetime of the low conductance state (Prod'hom et al., 1987). Fig. 6 compares traces and amplitude histograms obtained at pD 8.2 with 150 mM Na alone (top traces) and 150 mM Na + 10 mM Li (bottom traces). With Na alone, many of the transitions to the low conductance are long enough to be clearly resolved, whereas in the presence of 10 mM Li

those transitions are so short that they are no longer resolved and appear as large noise in the open channel. We compared signals of roughly similar amplitude and therefore chose a more negative potential for the Na/Li mixture, since Li decreases the conductance observed in Na alone (Fig. 5). The choice of different potentials is justified since we have shown in Fig. 1 that the kinetics of the proton-induced fluctuations are voltage independent, a conclusion which also holds for fluctuations induced by deuterons (data not shown). The shortening of the dwell times at the low conductance produced by the addition of 10 mM Li is also apparent from comparison of the amplitude histograms associated with each set of records. In Na alone, distinct peaks can be observed at each conductance level, whereas in the presence of 10 mM Li the peak of the low conductance has been transformed into a broad shoulder that is shifted to the right and fused with the peak of the high conductance. This is the expected finding for the situation in which filtering decreases the amplitude of very short events.

The results shown in Figs. 5 and 6 fit nicely with the hypothesis that occupancy of the channel by permeant ions destabilizes the low conductance conformation of the channel. The direct observation of effects of low concentrations of Li on k_{off} strongly implies that the effects of all monovalent cations on the kinetics of the proton-induced fluctuations are similar. Quantitatively however, the destabilization of the low conductance state by Li is more pronounced, such that in H_2O and 150 mM Li the proton-induced fluctuations are shifted into a frequency domain that escapes detection at the bandwidth of our measurements. In analogy, it is not surprising that currents carried by Ba ions, which bind even more strongly to the channel than Li (see e.g., Hess et al., 1986), should not be measurably affected by proton-induced current fluctuations.

Effect of External pH on Li and Ba Conductances

Since Li destabilizes the low conductance state much more than Na, we cannot resolve the proton-induced fluctuations. However, depending on the degree of the destabilization, we might still be able to see a decrease of the elementary current at low pH. We therefore compared the Li conductance at pH 9 and 6. We performed the same measurements on unitary Ba currents, which also lack discrete proton-induced fluctuations.

Li and Ba conductances were decreased very little between pH 9 and 6. In cell-attached patches, with 160 mM Li in the pipette, g_{Li} = 25.7 ± 2.46 pS (mean ± SEM) at pH 9, and 22.1 ± 1.63 pS at pH 6. With 110 mM Ba as charge carrier, g_{Ba} = 26.3 ± 1.00 at pH 9, and 22.2 ± 0.31 pS at pH 6. It is not clear whether this slight effect is related to the proton-induced fluctuations observed with the other monovalent charge carriers. However, we can use these measurements to obtain a lower limit estimate of the lifetimes of the low conductance level in Li and Ba. As in the companion paper (Pietrobon et al., 1989) we denote $k_{on} = 1/\tau_h$ and $k_{off} = 1/\tau_l$, where τ_h and τ_l are the mean lifetimes of the high and low conductance levels, respectively. The second-order on-rate (slope of k_{on} vs. a_H) does not change for Cs, K, and Na (Pietrobon et al., 1989) and we will therefore assume that it has the same value of $\sim 4 \times 10^{11}$ (/Ms) in the presence of Li or Ba. The relative proton-induced conductance change is also similar for Cs, K, and Na (~70%) and we assume that

this is also the amplitude of the proton-induced fluctuations with Li and Ba. With these assumptions, in order to get no more than a 10% reduction of the total elementary current at pH 6, k_{off} must be greater than 2.5×10^6/s. This corresponds to a lifetime of the low conductance level of 0.4 μs, evidently far too short to be apparent even as noise in our recordings. Since $k_{off} \approx 15{,}000$/s with Na (Pietrobon et al., 1989), Li and Ba must destabilize the low conductance state at least 100 times more than Na.

Ca Currents in Physiological Solutions Do Not Show Proton-induced Conductance Fluctuations

The remaining question concerns the existence of proton-induced fluctuations of L-type Ca currents under physiological conditions, in the presence of 1.8 mM Ca. Following our arguments from the last sections we would anticipate that currents

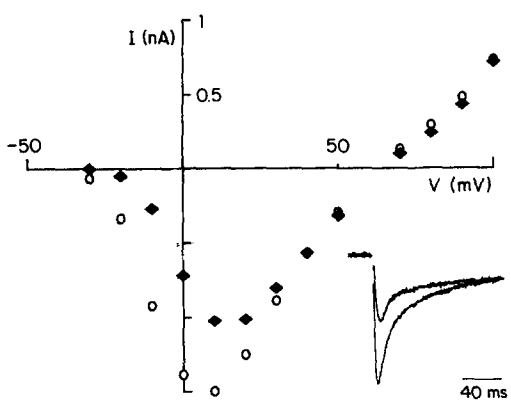

FIGURE 7. Whole-cell Ca currents and I-V relations at two different values of pH_o. Guinea pig ventricular myocyte. Na channels inactivated by the holding potential of −40 mV. *Circles*, peak currents at pH 7.5. *Diamonds*, peak currents after change of bath solutions to pH 6.5. The effect of pH_o was fully reversible (not shown). (*Inset*) Superimposed current traces obtained at pH_o 7.5 and 6.5. Test potential = 0 mV. Pipette solution (in millimolar): 135 CsCl, 10 EGTA, 10 HEPES, 4 ATP, 5 $MgCl_2$ at pH 7.5. Bath solution: 145 NaCl, 1.8 $CaCl_2$, 10 HEPES or MES, at pH 7.5 or 6.5.

carried by Ca should not show measurable fluctuations. We have already shown (Pietrobon et al., 1988) that a Ca ion in the pore destabilizes the low conductance, but we could not judge quantitatively the degree to which the equilibrium between the two conductances is biased toward the high conductance. To resolve the issue, we recorded whole-cell Ca currents with physiological concentrations of Ca and Na, since under these conditions single-channel currents are too small to be detected with high enough resolution. Ca currents were recorded from guinea pig ventricular cells. A holding potential of −40 mV was chosen, to assure that all Ca current would be carried by L-type channels (Bean 1985; Nilius et al., 1985; Mitra and Morad, 1986; Bonvallet, 1987; Hagiwara et al., 1988).

Fig. 7 shows superimposed current records obtained at pH_o 7.5 and 6.5 and the corresponding current-voltage (I-V) relations at the two pHs. Lowering the pH_o to 6.5 decreases the Ca current at negative potentials but has no effect on the peak currents positive to ~+10 mV. In particular the conductance of the descending limb of the I-V curve is not changed. The unaltered macroscopic conductance

strongly suggests that the single-channel conductance is not changed over the pH range 7.5–6.5. Instead, the effects of pH_o can be explained by the well documented shift of the activation curve towards more positive potentials in low pH_o (Krafte and Kass, 1988). This shift is due to a proton-related change in surface potential, which in the pH range tested in Fig. 7 affects channel gating but not permeation (Krafte and Kass, 1988). We have observed this shift at the single-channel level as well (data not shown), but it did not interfere with our measurements of the open-channel properties. In addition to the pH-induced shift of channel gating, Krafte and Kass (1988) also reported evidence for channel block in whole-cell recordings with Ca as charge carrier. However, block was only observed at pH < 5 and it is therefore not clear whether this is related to the pH-induced current fluctuations described here.

We conclude that L-type Ca currents carried by physiological [Ca] do not exhibit proton-induced conductance fluctuations at least down to a pH_o of 6.5. Thus this mechanism does not contribute to the modulation of the macroscopic Ca current by pH_o over the physiological pH range. Recently, Kaibara and Kameyama (1988) have shown that the inhibition of L-type Ca current by internal protons (e.g., Sato et al., 1985) is also predominantly accounted for by a change in channel gating and not channel conductance.

Kinetics of Proton-induced Fluctuations Vary with the Concentration of Permeant Ion

A direct test of our assertion that the kinetics of the proton-induced fluctuations are influenced by interactions of permeant ions with permeation sites consists of a kinetic analysis of the fluctuations under conditions of variable channel occupancy. The most direct way to change channel occupancy is to change the concentration of permeant ion. Fig. 8 shows that the equilibrium between the high and low conductance level at pH 8.4 is indeed altered when current traces are compared with 60, 160, or 320 mM K as permeant ion. This is apparent most directly from the amplitude histograms associated with the traces obtained with each value of [K]. For clarity, the peak of the closed channel at 0 pA is not included in the amplitude histograms. As [K] decreases, the channel spends progressively more time at the low conductance level and the corresponding peak of the amplitude histogram becomes proportionally larger.

Fig. 9 plots the rate constants of the transitions between the two conductances as a function of [K]. We find that the equilibrium, as expressed by $-\log k_{off}/k'_{on}$ ($k'_{on} = k_{on}/a_H$), decreases by 0.6 log units as [K] is increased from 60 to 320 mM. This is due to an increase of k_{off} and a decrease of k'_{on}. The change in k_{off} is consistent with the interpretation that the higher the occupancy of the channel, the more the low conductance state is destabilized. Since the differences between the kinetic values shown in Fig. 9 are small, their values, including tests for the level of statistical significance, are given in Table I.

The values of k'_{on} are also functions of [K] and decrease with increasing [K]. The rate-limiting step determining k_{on} is the association rate for protons (this is a model-independent conclusion based on the linear dependence of k_{on} and a_H; Pietrobon et al., 1989). The simplest explanation for the effect of [K] on k'_{on} is to say that in the

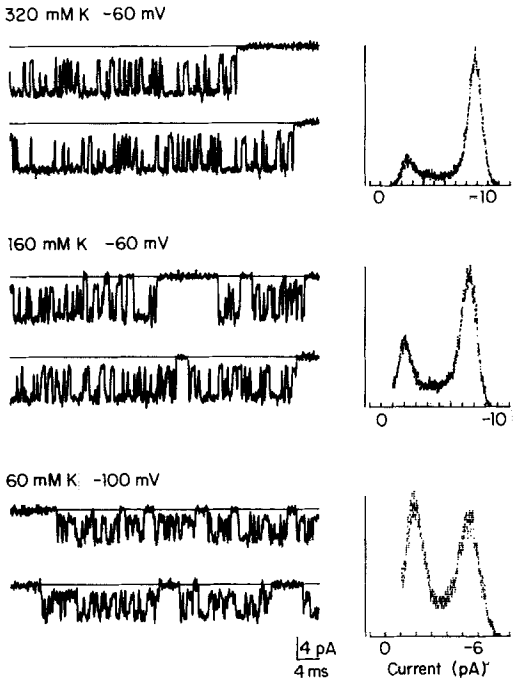

FIGURE 8. The concentration of the charge carrier biases the equilibrium between the two conductance states. Cell-attached recordings (*left*) with 320 (top traces), 160 (middle traces), and 60 mM potassium + 100 mM choline (bottom traces) at −60, −60, and −100 mV, respectively. Pipette pH 8.4. The amplitude histograms are shown on the right of the corresponding traces. The peak of the closed level at 0 pA has been omitted for clarity.

vicinity of the protonation site net negative charge gets screened progressively as the ionic strength is increased from 60 KCl plus sucrose to 160 and 320 KCl. The screening of the negative charge then decreases the association rate for protons and therefore k_{on}. This argument however does not explain why k'_{on} is also higher in 60 mM KCl plus 100 mM choline than in 160 mM KCl, since these two solutions have the same ionic strength. A possible resolution of the conflict may be found if one considers that although choline and K have the same charge, the much larger choline molecule might not be as effective as K in screening localized charges in the close vicinity of the protonation site.

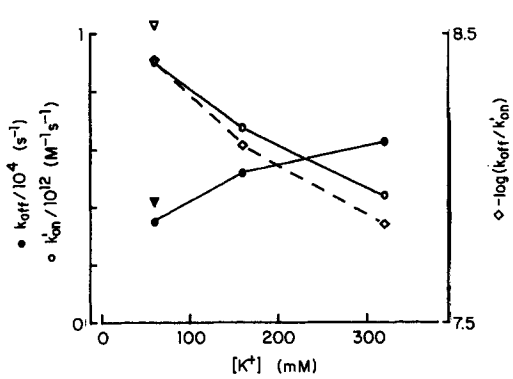

FIGURE 9. Kinetics of the proton-induced fluctuations as a function of [K]. $k'_{on} = k_{on}/a_H$ (*open circles*), k_{off} (*closed circles*), and $-\log(k_{off}/k'_{on})$ (*diamonds*) are plotted against the pipette potassium concentration. SEM are not shown because they were smaller than the size of the symbols. The lines connect points obtained with 60 mM K + 100 mM choline, 160, and 320 mM K. The single points for k'_{on} and k_{off} at 60 mM K were obtained with 60 mM K + 200 mM sucrose. Pipette pH 8.4. Cell-attached patches.

DISCUSSION

Mechanism of Permeation in L-Type Ca Channels

The results presented here and in the preceding paper (Pietrobon et al., 1989) extend our understanding of the mechanisms of permeation and ionic selectivity in L-type Ca channels. We can now compare conductances, reversal potentials, and affinities for the channel pore for a wide range of monovalent and divalent ions. It is clear that L-type Ca channels not only select among divalent ions on the basis of the ion's affinity for intra-channel binding sites (Almers and McCleskey, 1984; Hess and Tsien, 1984; Hess et al., 1986; Lansman et al., 1986; see also Hagiwara et al., 1974; Chesnoy-Marchais, 1985, Nelson, 1986 for other types of Ca channels), but that the same mechanism holds for selectivity among monovalent ions (Coronado and Smith 1987; Pietrobon et al., 1988; this paper). This is most evident if one compares the sequence of single-channel conductances, which increase in the order Ca ≈ Sr < Ba ≈ Li < Na < K < Cs, to the sequence of affinities which decrease in the same order. The relative affinities are obtained either by measurements of rever-

TABLE I

	$k'_{on}/10^{11}$	$k_{off}/10^3$	n
	$(M \cdot s)^{-1}$	s^{-1}	
160 mM KCl	6.80 ± 0.40	5.23 ± 0.15	4
320 mM KCl	4.44 ± 0.40 $P < 0.001$	6.77 ± 0.90 $P < 0.01$	7
60 mM KCl + 100 mM choline-Cl	9.01 ± 1.13 $P < 0.005$	3.48 ± 0.34 $P < 0.001$	7
60 mM K^+ + 200 mM sucrose	10.32 ± 0.47 $P < 0.001$	4.19 ± 0.66 $P < 0.02$	5

$k'_{on} = k_{on}/a_H$. n = number of patches. The statistical level of significance P was obtained by Student's t test. The reference value for each comparison was the one for 160 mM KCl.

sal potentials (Hess et al., 1986; Coronado and Smith, 1987; Pietrobon et al., 1988), or more directly by comparing the half-saturation point of conductance-concentration curves (Hess et al., 1986; Figs. 3 and 4 of this paper) or the direct interaction of two ions in mole fraction experiments (Almers and McCleskey, 1984; Hess and Tsien, 1984; Fig. 5 of this paper). The very high selectivity for divalent over monovalent ions is achieved by an affinity for divalent ions which greatly exceeds that for monovalent ions. Thus multiple occupancy and ion-ion interactions are observed for divalent ions, for example as anomalous mole fraction effects (Eisnman et al., 1967) in mixtures of Ca and Ba (Almers and McCleskey, 1984; Hess and Tsien, 1984). In contrast, even the most tightly binding monovalent ions seem not to interact with each other in the pore, a conclusion drawn from the lack of an anomalous mole fraction effect in mixtures of Na and Li (Fig. 5).

Comparison of the pH Effects and Monovalent Permeabilities in Various Ca Channel Types

We have observed the reported effects of protons on L-type Ca channels from all three cell types we investigated. The cells include the ones studied in this paper,

namely cardiac ventricular myocytes and undifferentiated PC-12 cells, as well as Swiss 3T3 fibroblasts (Chen, C., and P. Hess, unpublished data). The conductances for monovalent ions as well as the proton-induced current fluctuations are indistinguishable in the L-type Ca channels of these three cells and are therefore most likely a general property of all L-type Ca channels. For the reasons given below, we restrict the use of the denomination "L-type" Ca channel to nonskeletal muscle DHP-sensitive Ca channels.

Coronado and Affolter (1986) and Coronado and Smith (1987) have investigated monovalent permeabilities in DHP-sensitive Ca channels from skeletal muscle T-tubular membranes incorporated into lipid bilayers. The T-tubular Ca channels share monovalent permeability in the absence of divalent ions with the L-type Ca channels, and they show a similar selectivity and affinity sequence for monovalent cations (Coronado and Smith, 1987), but they differ significantly from the L-type Ca channels in the detailed properties of monovalent permeation. The conductances of the T-tubular Ca channels range from 18 pS with Li to 30 pS with Cs, whereas the corresponding conductances of the L-type Ca channel range from 25 pS with Li to 175 pS with Cs. A direct comparison of the results obtained with the two channel types is somewhat hampered by the fact that we measure conductances from the linear I–V of inward currents whereas Coronado and Smith (1987) obtained their conductance measurements from outward currents. We have found that the conductance for Na is equal for inward and outward currents (Fig. 2 and unpublished data), whereas the conductance for Cs is smaller for outward than inward currents (unpublished data). Nevertheless, even when conductances of outward currents are compared, the values for the L-type Ca channels considerably exceed those of the skeletal muscle Ca channel. It is not clear whether the mechanism of proton-induced fluctuations is also present in the T-tubular Ca channels, because all published records of monovalent unitary currents are obtained from outward currents (Coronado and Affolter, 1986; Coronado and Smith, 1987), which do not show clear proton-induced fluctuations even in the L-type Ca channel (Fig. 2). In any case, the frequency limitations imposed by bilayer recordings (100–500 Hz) would be expected to severely attenuate the rapid proton-induced fluctuations.

Another difference between skeletal and nonskeletal muscle DHP-sensitive Ca channels concerns the presence of negative surface charge close to the external entry of the permeation pathway. Coronado and Affolter (1986) conclude that in skeletal muscle channels no net surface charge on the protein itself is close to the channel entry and that the effect of the charge on the lipid should be minimal in native membranes. In contrast, we find that permeant ions must experience a substantial surface potential when they enter the L-type channel, as evidenced by the different shapes of the conductance-activity plots under conditions of constant or varying ionic strength.

The functional differences between the permeation of DHP-sensitive Ca channels from skeletal muscle and nonskeletal muscle origin (in addition to the marked differences in gating kinetics) further emphasize that the two channels may also be significantly different at the structural level (see also Rosenberg et al., 1986; Ma and Coronado, 1988).

Konnerth et al. (1987) and Davies et al. (1988) have recently described a different effect of protons, which the authors interpret as a transformation of a Ca channel from its Ca-conducting, voltage-activated state into a Na-conducting, nonvoltage-dependent state. The proton-induced "transformed" current activates in response to a rapid step decrease of pH_o and relaxes within several seconds. The authors do not explicitly say which type of Ca channel is being transformed. We can say with certainty that the phenomenon of proton-induced fluctuations which we describe in this and previous papers is not related to the effect of Konnerth et al. (1987) and Davies et al., (1988). Our measurements are obtained at a maintained pH and are apparent over the whole pH range of 6–9. Contrary to the assertion of Davies et al. (1987), that the single-channel properties of their proton-induced currents are similar to those of Na currents flowing through high-threshold (L-type) Ca currents in the absence of divalent ions, their proton-activated channel in symmetrical Na is unaffected by a change in proton activity between pH 5.7 and 7.3. This is in strict contrast to the pH sensitivity of the channel amplitude observed under similar ionic conditions for the L-type Ca channel (Prod'hom et al., 1987, Pietrobon et al., 1989). The L-type Ca channel remains DHP sensitive and voltage gated when it conducts monovalent ions, whereas the proton-activated current is not. In addition, proton-activated currents cannot be elicited in cardiac cells (Davies et al., 1988), whereas the monovalent currents and the proton-induced current fluctuations are identical in L-type Ca currents from cardiac and noncardiac cells. Based on these arguments, we suggest that the proton-induced currents observed by Konnerth et al. (1987) and Davies et al. (1988) are not related to L-type Ca channels. It remains to be seen whether these currents are carried by another type of Ca channel, or whether they represent a proton-activated nonselective cation channel as originally proposed by Kristhal and Pidoplichko (1980, 1981).

Interactions between Permeant Ions and the Channel Protein

The observation that permeant ions destabilize the lifetime of the low conductance state suggests that the binding of a permeant ion inside the channel changes the channel conformation. This should not be surprising, because the selectivity sequence of the intra-channel binding sites and their high affinity for Ca (dissociation constant of ~1 μM) are typical for multi-ligand binding sites in which the metal ion is coordinated by six or more groups with net or partial negative charge. The size of the coordinating cavity must be quite flexible, since it can very effectively chelate the Ca ion (2.0 Å) but also bind Cs (ionic diameter, 3.5 Å). Since the coordinating groups are likely to be contributed by different membrane-spanning regions of the protein surrounding the central pore, one can easily imagine that the electrostatic interactions between the ion and the coordinating groups lead to a slight rearrangement of the tertiary structure of at least some part of the protein. Our results suggest that the physiological ion, Ca, forms a stabilizing complex with the channel protein. In the absence of Ca, this stabilizing effect is lost and the channel protein can assume a variety of other conformations, one of which we detect electrically as the low conductance state.

The importance of this ion-channel interaction for the mechanism of selectivity cannot be judged from our results. We have correlated channel occupancy with the

extent of destabilization of the low conductance state. However, we cannot determine absolute channel occupancies and therefore can not exclude that the more strongly binding ions do not just occupy the site for a longer time but also interact with it in an ion-specific way. If such ion-specific interactions existed, one could imagine that an ion leaves the channel in a state that is relatively less favorable for the permeation of a competing ion. For such a mechanism to contribute to selectivity, the conformational change produced by one ion must last long enough to be felt by the next ion. Models of energy profiles with fluctuating barriers have been proposed (Ciani, 1984; Lauger, 1985) to account for permeation in channels with such properties.

Location of Protonation Site and Mechanism Underlying Conductance Change

Before we can interpret the observed lack of voltage dependence of k_{on} and k_{off} (Fig. 1), we must consider the relationship between k_{on} and k_{off} and the protonation/

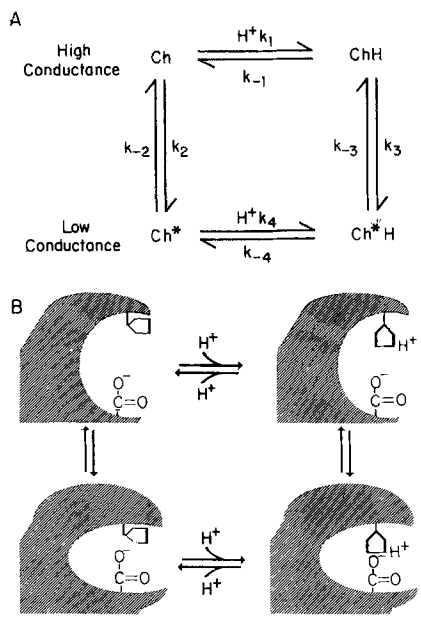

FIGURE 10. Four-state model of the protonation cycle (*A*) and possible physical representation of the protonation site on an external domain of the channel protein (*B*).

deprotonation rate constants. In our four-state model (Pietrobon et al., 1989, and see Fig. 10), changes of the protonation or deprotonation rate constants lead to complicated changes in the measured rate constants k_{on} and k_{off}. For example, with the set of rate constants that give a good fit to our data (Pietrobon et al., 1989), changes in the protonation and deprotonation rate both change the value of k_{on}. k_{on} increases with an increasing rate of protonation but decreases with an increasing rate of deprotonation. The value of k_{off} is less sensitive to the kinetics of the protonation reaction because its value is determined mainly by the rate of the conformational change (k_{-2} and k_{-3}). In theory, the observed lack of voltage dependence of

k_{on} and k_{off} (Fig. 1) could result from a concomitant change of both protonation and deprotonation rate constant. The two effects could effectively cancel each other with no net change in k_{on}. However, we consider this special case very unlikely. Regardless of the particular model, different sets of rate constants are needed to simulate the data with the three different permeant ions (Cs, K, Na). In any model, the combined change in the protonation and deprotonation rate constants that would lead to no net change in k_{on} and k_{off} for one ion will lead to measurable changes in the proton-induced fluctuations for the other two ions. Because we could not detect any voltage dependence of k_{on} and k_{off} with either ion and at all pH values tested, we conclude that the protonation and deprotonation rate constants themselves are also voltage independent.

The voltage independence of the protonation and deprotonation events and the exclusive accessibility of protons to the site from the external side of the channel strongly suggest a location of the protonation site on the external surface of the channel protein, outside of the transmembrane electric field.

We can further distinguish between two general locations. The site could be located close to the entrance of the permeation pathway, or far enough that entering ions do not experience the altered surface potential that must accompany protonation/deprotonation event. We exclude the former location on the following grounds: the plot of conductance vs. [K] has the same shape for the high and low conductance, both at constant and at varying ionic strength. This means that the entering ions do not feel an altered local surface potential caused by the changing charge at the protonation site. If they did, we would expect the point of half saturation to shift towards higher [K] for the low conductance (mainly protonated) state, but if anything, we observe the opposite trend (Fig. 3). Also, we would expect to see an increase of the difference between the two conductance levels at low ionic strength. The conclusion of a location of the protonation site far from the permeation pathway fits very nicely with our previous observation (Pietrobon et al., 1988), that a Ca ion enters the channel with equal probability whether it is in the high or low conductance state. A location of the protonation site far from the permeation path also means that protons cause the conductance change indirectly by promoting a conformational change of the channel protein. This is the main justification for choosing a model with four states, in which the channel can be protonated and deprotonated both at the high and low conductance level (see Pietrobon et al., 1989 and the next section).

We cannot pinpoint the mechanism by which the proton-induced conformational change decreases channel conductance, nor do we know which site or sites in the permeation path are linked allosterically to the protonation site. However, under the simplifying assumption that channel occupancy at a discrete permeation site is controlling the conformational change, the relevant site must be situated at a location in the channel where a permeant ion crosses a similar electrical distance as it enters and leaves the site. In this case a change in membrane voltage will accelerate or slow down the access to and exit from that site by a similar factor and the average occupancy of the site will be voltage independent. This postulate is needed to explain the experimental finding of voltage-independent kinetics of the proton-induced fluctuations, if indeed they are influenced by channel occupancy.

A Possible Physical Representation of the Protonation Site

In the preceding paper (Pietrobon et al., 1989) we have introduced a formal model of the protonation cycle, which is shown in Fig. 10 *A*. There are two proton equilibria with pK values of 6.3 and 9.3 (Pietrobon et al., 1989) associated with the high and low conductance, respectively. The difference in the two pK values is mostly caused by different deprotonation rate constants. We must therefore find a mechanism, whereby a change in protein conformation greatly changes the stability of the protonated state. This leaves us with two possibilities for a physical interpretation. Either the protonation group is a lysine residue (pK in polypeptide chain = 10.4, see Creighton, 1984) whose protonated $-NH_3^+$ group becomes destabilized in the high conductance channel, or it is a histidine residue (pK 6.2) whose protonated positively charged imidazole ring becomes stabilized in the low conductance channel. We do not consider cysteine (pK 9.1–9.5) or tyrosine (pK 9.7) because their protonated forms are uncharged and it is therefore very difficult to conceive of a mechanism that would shift the pK to lower values primarily through a destabilization of the protonated state.

Changes of pK values by three pH units are very large and must involve short range electrostatic interactions. A diagrammatic representation of the protonation cycle involving a histidine is shown in Fig. 10 *B*. The histidine is located near a negatively charged carboxyl group. In the high conductance states, the two groups are sufficiently far from each other that there are no direct interactions, thus protonation and deprotonation rate constants have values appropriate for a pK of 6.3. The conformational change to the low conductance level brings the two groups much closer together, such that a salt bridge forms between the positively charged protonated histidine and the negatively charged carboxyl group. This greatly stabilizes the protonated state. Although the conformational change to the low conductance state can take place from the unprotonated or protonated state, it occurs much more readily from the protonated state ($k_3 \gg k_2$). This implies that the electrostatic attraction between the two charged residues lowers the activation energy for the transition between the two conformations. As mentioned in the preceding paper (Pietrobon et al., 1989), to satisfy microscopic reversibility, the protonation rate constant in the low conductance conformation ($a_H k_4$) has to be higher than the one at the high conductance ($a_H k_1$). Within the framework of this physical representation, the higher value of $a_H k_4$ is actually expected, because at the low conductance an incoming proton would be attracted more by the negative charge from the neighboring carboxyl group.

We thank Dr. Mark Plummer for help with tissue culturing.

This work was supported by a National Institutes of Health grant HL-37124, the Lucille P. Markey Charitable Trust, fellowships from European Molecular Biology Organization and Fogarty (D. Pietrobon), and a fellowship from the Muscular Dystrophy Association (B. Prod'hom).

Original version received 16 September 1988 and accepted version received 11 January 1989.

REFERENCES

Almers, W., and E. W. McCleskey. 1984. Non-selective conductance in calcium channels of frog muscle: calcium selectivity in a single-file pore. *Journal of Physiology.* 353:585–608.

Apell, H. J., E. Bamberg, and P. Lauger. 1979. Effects of surface charge on the conductance of the gramicidin channel. *Biochimica et Biophysica Acta.* 552:369–378.

Bean, B. P. 1985. Two kinds of calcium channels in canine atrial cells. Differences in kinetics, selectivity, and pharmacology. *Journal of General Physiology.* 86:1–30.

Bonvallet, R. 1987. A low threshold calcium current recorded at physiological Ca concentration in single frog atrial cells. *Pflügers Archiv.* 408:540–542.

Cavalie, A., R. Ochi, D. Pelzer, and W. Trautwein. 1983. Elementary currents through Ca^{2+} channels in guinea pig myocytes. *Pflügers Archiv.* 398:284–297.

Chesnoy-Marchais, D. 1985. Kinetic properties and selectivity of calcium-permeable single channels in *Aplysia* neurones. *Journal of Physiology.* 367:457–488.

Ciani, S. 1984. Coupling between fluxes in one-particule pores with fluctuating energy profiles. *Biophysical Journal.* 46:249–252.

Coronado, R., and H. Affolter. 1986. Insulation of the conduction pathway of muscle transverse tubule calcium channels from the surface charge of bilayer phospholipid. *Journal of General Physiology.* 87:933–953.

Coronado, R., and J. S. Smith. 1987. Monovalent ion current through single calcium channels of skeletal muscle transverse tubules. *Biophysical Journal.* 51:497–502.

Cota, G., and E. Stefani. 1984. Saturation of calcium channels and surface charge effects in skeletal muscle fibers of the frog. *Journal of Physiology.* 351:135–154.

Creighton, T. E. 1984. Proteins. W. H. Freeman and Company, New York. 515 pp.

Dani, J. A. 1986. Ion-channel entrances influence permeation. *Biophysical Journal.* 49:607–618.

Dani, J. A., and G. Eisenman. 1987. Monovalent and divalent cation permeation in acetylcholine receptor channels. *Journal of General Physiology.* 89:959–983.

Davies, N. W., H. D. Lux, and M. Morad. 1988. Site and mechanism of activation of proton-induced sodium current in chick dorsal root ganglion neurones. *Journal of Physiology.* 400:159–187.

Eisenman, G., J. P. Sandblom, and J. L. Walker. 1967. Membrane structure and ion permeation. *Science.* 155:965–974.

Fenwick, E. M., A. Marty, and E. Neher. 1982. Sodium and calcium channels in bovine chromaffin cells. *Journal of Physiology.* 331:599–635.

Fukushima, Y., and S. Hagiwara. 1985. Currents carried by monovalent cations through calcium channels in mouse neoplastic B lymphocytes. *Journal of Physiology.* 358:255–284.

Hagiwara, N., H. Irisawa, and M. Kameyama. 1988. Contribution of two types of calcium currents to the pacemaker potentials of rabbit sino-atrial node cells. *Journal of Physiology.* 395:233–253.

Hagiwara, S., J. Fukuda, and D. C. Eaton. 1974. Membrane currents carried by Ca, Sr, and Ba in barnacle muscle fiber during voltage clamp. *Journal of General Physiology.* 63:564–578.

Hamill, O. P., A. Marty, E. Neher, B. Sakmann, and F. J. Sigworth. 1981. Improved patch-clamp techniques for high-resolution current recording from cells and cell-free membrane patches. *Pflügers Archiv.* 391:85–100.

Hess, P., J. B. Lansman, and R. W. Tsien. 1986. Calcium channel selectivity for divalent and monovalent cations. Voltage and concentration dependence of single channel current in ventricular heart cells. *Journal of General Physiology.* 88:293–319.

Hess, P., and R. W. Tsien. 1984. Mechanism of ion permeation through calcium channel. *Nature.* 309:453–456.

Hille, B. 1984. Ionic channels of excitable membranes. Sinauer Associates, Sunderland, MA. 426 pp.

Hille, B., and W. Schwartz. 1978. Potassium channels as multi-ion single-file pores. *Journal of General Physiology.* 72:409–442.

Kaibara, M., and M. Kameyama. 1988. Inhibition of the calcium channel by intracellular protons in single ventricular myocytes of the guinea pig. *Journal of Physiology.* 403:621–640.

Konnerth, A., H. D. Lux, and M. Morad. 1987. Proton-induced transformation of calcium channel in chick dorsal root ganglion cells. *Journal of Physiology.* 386:603–633.

Krafte, D. S., and R. S. Kass. 1988. Hydrogen ion modulation of Ca channel current in cardiac ventricular cells. Evidence for multiple mechanisms. *Journal of General Physiology.* 91:641–657.

Krishtal, O. A., and V. I. Pidoplichko. 1980. A receptor for protons in the nerve cell membrane. *Neuroscience.* 5:2325–2327.

Krishtal, O. A., and V. I. Pidoplichko. 1981. A receptor for protons in the membrane of sensory neurones may participate in nociception. *Neuroscience.* 6:2599–2601.

Lansman, J. B., P. Hess, and R. W. Tsien. 1986. Blockade of current through single calcium channels by Cd^{2+}, Mg^{2+}, and Ca^{2+}. Voltage and concentration dependence of calcium entry into the pore. *Journal of General Physiology.* 88:321–347.

Lauger, P. 1985. Ionic channels with conformational substrates. *Biophysical Journal.* 47:581–591.

Ma, J., and R. Coronado. 1988. Conductance-activity, current-voltage, and mole fraction relationships for calcium, barium, and sodium in the T tubule calcium channel. *Biophysical Journal.* 53:556*a*. (Abstr.)

Mitra, R., and M. Morad. 1986. Two types of calcium channels in guinea pig ventricular myocytes. *Proceedings of the National Academy of Sciences.* 93:5340–5344.

Nelson, M. 1986. Interactions of divalent cations with single calcium channels from rat brain synaptosomes. *Journal of General Physiology.* 87:201–222.

Nilius, B., P. Hess, J. B. Lansman, and R. W. Tsien. 1985. A novel type of cardiac calcium channel in ventricular cells. *Nature.* 316:443–446.

Perrin, D. D., and B. Dempsey. 1974. Buffers for pH and metal ion control. Chapman and Hall Ltd., London. 182 pp.

Pietrobon, D., B. Prod'hom, and P. Hess. 1988. Conformational changes associated with ion permeation in L-type calcium channel. *Nature.* 333:373–376.

Pietrobon, D., B. Prod'hom, and P. Hess. 1989. Interactions of protons with single open L-type calcium channels. pH dependence of proton induced current fluctuations with Cs^+, K^+, and Na^+ as charge carriers. *Journal of General Physiology.* 94:00–00.

Prod'hom, B., D. Pietrobon, and P. Hess. 1987. Direct measurement of proton transfer rates to a group controlling the dihydropyridine-sensitive Ca^{2+} Channel. *Nature.* 329:243–246.

Rosenberg, R. L., P. Hess, R. W. Tsien, H. Smilowitz, and J. P. Reeves. 1986. Calcium channels in planar lipid bilayers: insights into mechanisms of ion permeation and gating. *Science.* 231:1564–1567.

Sato, R., A. Noma, Y. Kurachi, and H. Irisawa. 1985. Effects of intracellular acidification on membrane currents in ventricular cells of the guinea-pig. *Circulation Research.* 57:553–561.

Urban, B. W., S. B. Hladky, and D. A. Haydon. 1987. Ion movements in gramicidin pores. An example of single-file transport. *Biochimica et Biophysica Acta.* 602:331–354.

Wilson, D. L., K. Morimoto, Y. Tsuda, and A. M. Brown. 1983. Interaction between calcium ions and surface charge as it relates to calcium currents. *Journal of Membrane Biology.* 72:117–130.

Yatani, A., J. Codina, Y. Imoto, J. P. Reeves, L. Birnbaumer, and A. M. Brown. 1987. A G protein directly regulates mammalian cardiac calcium channels. *Science.* 238:1288–1292.